Seasonality as a driver of pH1N12009 influenza vaccination campaign impact

Kirsty J. Bolton[a,*], James M. McCaw[b,c], Mathew P. Dafilis[c], Jodie McVernon[d], Jane M. Heffernan[e]

[a]*School of Mathematical Sciences, University of Nottingham, University Park, Nottingham, NG7 2RD, UK*
[b]*School of Mathematics and Statistics, The University of Melbourne, Parkville, Australia*
[c]*Centre for Epidemiology and Biostatistics, Melbourne School of Population and Global Health, The University of Melbourne, Parkville, Australia*
[d]*Peter Doherty Institute for Infection and Immunity, The Royal Melbourne Hospital and The University of Melbourne, Parkville, Australia*
[e]*Centre for Disease Modelling, Mathematics & Statistics, York University, Canada*

Abstract

Although the most recent respiratory virus pandemic was triggered by a Coronavirus, sustained and elevated prevalence of highly pathogenic avian influenza viruses able to infect mammalian hosts highlights the continued threat of pandemics of influenza A virus (IAV) to global health. Retrospective analysis of pandemic outcomes, including comparative investigation of intervention efficacy in different regions, provide important contributions to the evidence base for future pandemic planning. The swine-origin IAV pandemic of 2009 exhibited regional variation in onset, infection dynamics and annual infection attack rates (IARs). For example, the UK experienced three severe peaks of infection over two influenza seasons, whilst Australia experienced a single severe wave. We adopt a seasonally forced 2-subtype model for the transmission of pH1N12009 and seasonal H3N2 to examine the role vaccination campaigns may play in explaining differences in pandemic trajectories in temperate regions. Our model differentiates between the nature of vaccine- and infection-acquired immunity. In particular, we assume that immunity triggered by infection elicits heterologous cross-protection against viral shedding in addition to long-lasting neutralising antibody, whereas vaccination induces imperfect reduction in susceptibility. We employ an Approximate Bayesian Computation (ABC) framework to calibrate the model using data for pH1N12009 seroprevalence, relative subtype dominance, and annual IARs for Australia and the UK. Heterologous cross-protection substantially suppressed the pandemic IAR over the posterior, with the strength of protection against onward transmission inversely correlated with the initial reproduction number. We show that IAV pandemic timing relative to the usual seasonal influenza cycle influenced the size of the initial waves of pH1N12009 in temperate regions and the impact of vaccination campaigns.

Keywords: pandemic influenza, vaccination, influenza seasonality

1. Introduction

Influenza A (IAV) pandemic viruses, characterised by their high transmissibility and novel genetic material, spread rapidly through a population due to low population-average immunological protection, quickly replacing seasonal viruses [12]. Pandemics triggered by IAV remain a threat to human health. Of recent concern are several clades of highly pathogenic avian H5N1 IAV that have

*Corresponding author, kirsty.bolton@nottingham.ac.uk

caused widespread disease in wild and farmed birds [29]. Although the extent to which the virus is adapting to mammalian host receptors is uncertain [80], there is evidence of spillover to multiple mammalian hosts [29, 80]. In 2009, seasonal H1N1 viruses were displaced by a triple reassortant swine-origin H1N1 virus (henceforth pH1N12009). Prior to the emergence of pH1N12009, neutralising antibody (NAb) to this virus were present primarily in older adults with overall prevalence observed to be similar across many regions worldwide [10]. As for other historical pandemic outbreaks, multiple waves of infection were observed [57, 83]. However, there were marked differences between epidemic patterns in different regions (Figure 1, [86]).

In Australia, the pandemic was largely characterised by one distinct 10–12 week wave of infection that occurred during the typical influenza season months [5, 82], and this was followed by a second wave of infection, observed one year later in the usual window for seasonal influenza activity, but with much reduced magnitude [82]. In Australia the first cases of pH1N12009 were identified in late April. Community transmission was established in early June, it peaked in mid-July, and largely resolved by late-September [5], with some differences in timing between individual states [7]. The overall IAR during the 2009 outbreak in Australia, estimated via the rise in prevalence of Ab titres above 40 (measured via haemaglutination inhibition assays), was up to $\approx 20\%$ [26, 54] (similar to that seen in neighbouring New Zealand, [6]).

In the UK, the pandemic was predominantly characterised by a wave of infection over the spring and early summer months of 2009, followed by another wave over the 2009–2010 influenza season. The first pandemic wave in the UK peaked in late July and receded after the start of the summer school holidays [85], generating IARs of around 30 per cent amongst children in high incidence areas [56]. The epidemic was reestablished alongside the resumption of school term in September [42]. Most countries in the Northern Hemisphere experienced a mild wave of infection in the second year following emergence, in the usual window for seasonal activity [47]. In contrast, the UK experienced another large outbreak over the 2010–11 season [60].

Travel links can somewhat synchronise influenza epidemics across neighbouring countries, but even with frequent air-travel, epidemics are not synchronised globally [59]. The determinants of variations in pandemic experience are unclear and likely multifactorial. Multi-strain dynamical systems tracking host infection history display complex dynamics [30, 65], suggesting differences in host immune profiles may be at play. Geographical heterogeneity in immune profiles could also be driven by differences in the uptake of seasonal and pandemic vaccination [17, 40, 69, 84, 89], differences in vaccine efficacy with nationally-adopted formulations [1, 40], and global variations in age-dependent mixing [63], either alone or in concert with age-dependent variation in vaccine uptake and/or efficacy [7, 37, 53, 85]. Pandemic influenza circulation is also likely to be influenced by local climatic effects including the effect of temperature and humidity on host immunity, mixing and virus survival [68, 72, 74].

We focus on the extent to which regional differences in vaccination campaign timing may drive these differences. In Australia the vaccination campaign began on September 30th 2009 [7]. In the UK vaccination for health-care workers and their patients began on the 21st October, with phase 2 of the rollout extending to young children beginning in mid-November [34]. A systematic review of vaccine efficacy indicates that unadjuvanted vaccines (such as Panvax adopted in Australia [55]) reduced risk of laboratory confirmed pH1N12009 infection by 80% (95% CI: $59\% - 90\%$). Adjuvanted vaccines (such as the GSK's Pandemrix AS03 adjuvanted vaccine used in the UK [43]) had lower overall efficacy against laboratory confirmed infection, and efficacy of adjuvanted vaccines was higher amongst children 66% (95% CI: $47\% - 78\%$) [43]. In future pandemics, deployment of vaccines for a novel IAV may be possible within ≈ 100 days with mRNA vaccines, which don't require the time intensive step of growing large quantities of virus [41]. Fast-tracked

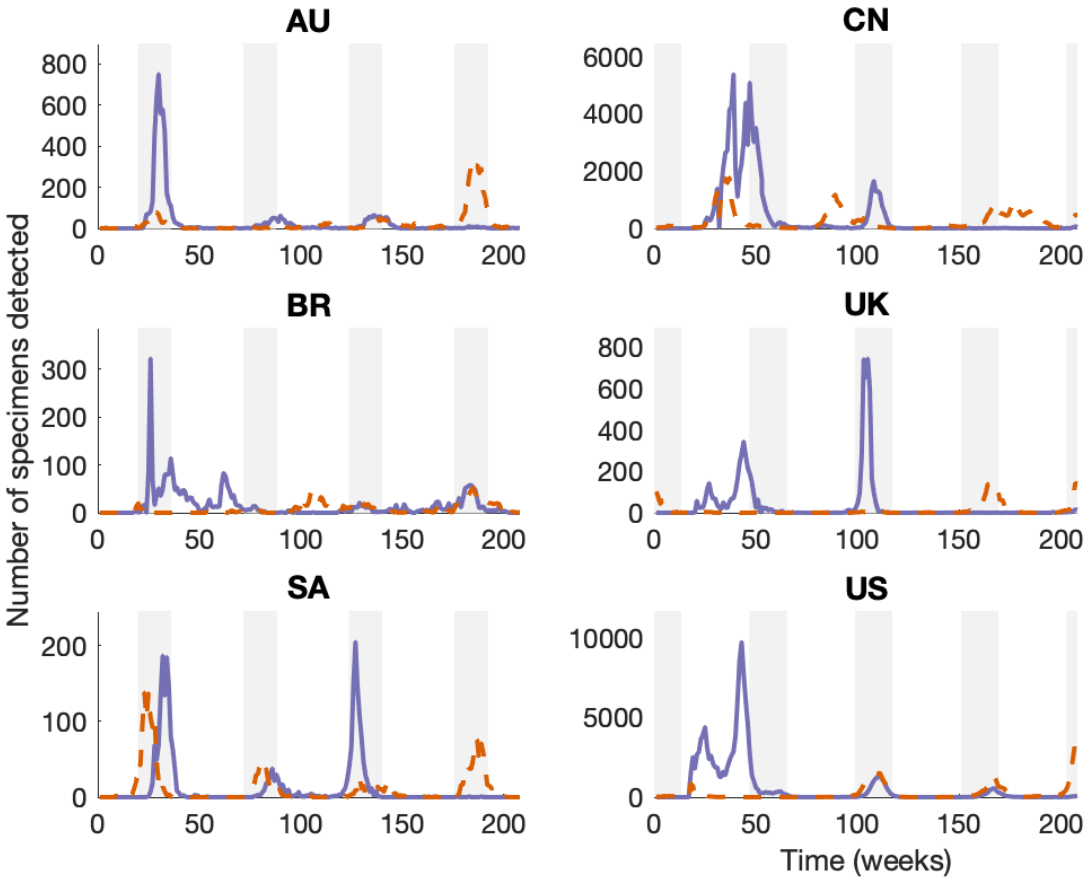

Figure 1: Influenza reporting in the Northern and Southern Hemispheres. The number of pH1N12009 (purple) and H3N2 (orange) specimens detected in Australia, Brazil, South Africa, China, the UK and the USA are shown, from January 2009 to Dec 2012. The shaded regions indicate the typical influenza peak seasons in both hemispheres.

production of licensed subunit IAV vaccines may also expedite rollout of a pandemic vaccine [70]. The development of higher efficacy vaccines may be possible through mRNA platforms that include multiple IAV proteins, or other next generation platforms perhaps in combination with the use of adjuvants [76].

In this paper, we describe a mathematical model for the spread of pandemic influenza that captures many possible time-dependent influences on pandemic IAV transmission: the timing of vaccination campaigns, waning of vaccine-induced immunity, acquisition and loss of sterilising and cross-protective immunity from natural infection, circulation of a competing resident seasonal IAV subtype, seasonal forcing and seasonal importation of cases. We focus on IAV circulation in approximately polar opposite countries with (largely) temperate climates: Australia and the United Kingdom. We use Approximate Bayesian Computation, with distance measure based on serological surveys of pandemic H1N1 circulation and seasonal H3N2 during and following the pandemic and data on relative subtype prevalence from sentinel surveillance, to calibrate our model and generate candidate parameter sets. Candidate parameter sets are then used to explore extent to which the timing of pandemic emergence with respect to seasonal drivers influences the impact of realised and hypothetical pandemic influenza vaccination programs on future waves of pandemic and seasonal IAV infection.

2. Materials and Methods

2.1. Influenza transmission model

We model the spread of pH1N12009 in concert with the seasonal H3N2 subtype from the emergence of pH1N12009 in April 2009 ($t = 0$) until April 2014. We have designed a two-subtype Susceptible-Infected-Recovered-Susceptible (SIRS) model that can describe and track the presence of protective NAb from a natural infection, partially protective cross-reactive immune responses, and vaccine induced protection, for each subtype. Each of the N hosts is assigned to one of a number of susceptible states S_{nm} where n (m) denotes the nature of susceptibility to subtype a (b). Indices are defined as 1: full susceptibility, ρ_a: vaccine-induced protection only, ϵ_{Sa}: heterologous cross-protection only, χ_a: vaccine-induced protection with heterologous cross-protection, 0: infection-induced reduction in susceptibiity with heterologous cross-protection and 0_s: infection-induced reduction in susceptibility from infection without heterologous cross-protection (see also the model schematic in Figure 2). The infectious period is assumed to have an average duration of 2.7 days [77]. Following recovery from infection, hosts migrate to a different susceptible state that reflects the impact of infection on their susceptibility to each subtype as depicted in Figure 2 and formalised in equation (A.1). In brief, natural infection with subtype i confers long-lasting neutralising protection to subtype i for an average time period $1/\phi_{D,i}$, following which strain turnover due to antigenic drift renders protective antibody to this subtype redundant [67]. Infection with subtype i also provides shorter lived cross-subtype protection that reduces a host's potential infectiousness by a factor ϵ_I. This feature is motivated by human challenge studies indicating influenza specific cytotoxic T cells [51] aid viral clearance, and household studies noting lower rates of symptomatic PCR-confirmed IAV for those with serum influenza-specific $CD8^+$ T-cells [31].

We assume that cross-subtype protection decays over a time-scale of $1/\phi_X = 2$ years, motivated by individual-level longitudinal data measuring the ability of serum cytotoxic T cells to lyse IAV infected cells [52]. Vaccination is assumed to reduce subtype-specific susceptibility by a factor ρ_i. Protection induced by vaccination is assumed to be lost over a time-scale $1/\phi_{V,i}$, independently of the rate of loss of naturally acquired sterilising or partially protective immunity. We assume that the population mixes homogeneously and both subtypes have the same basic reproduction number (in the absence of seasonal forcing), $\mathcal{R}_0$, however differences in the effective reproduction number between subtypes arise due to differences in the population immune profile to each subtype, driven initially by parameters in Table B.1. Infection with one subtype excludes concurrent infection with the other subtype.

We model transmission in each hemisphere by introducing a sinusoidal seasonal forcing term with timing determined by θ_{offset}. Transmission is enhanced maximally in winter for each hemisphere by a factor d_i. The importation of external cases n_i, which modifies the force of infection when added to $I_{\text{tot},i}$, is modelled by a constant forcing term modified by an additive sinusoidal term with opposite phase to the seasonal forcing, capturing air-travel from an epidemic in the opposite hemisphere, $n_i = N(c_i - s_i \cos[2\pi(t/1 \text{ year}) - \theta_{\text{offset}}])$.

Throughout this work we assume subtype a corresponds to pH1N12009 IAV and subtype b seasonal H3N2 IAV, and will sometimes use these labels on subtype dependent parameters when emphasising the application of this model to post-2009 IAV circulation. We assume vaccines are distributed over 3 month intervals for both seasonal and pandemic vaccination campaigns. The rate of vaccination against pH1N12009 alone (v_a) is chosen to provide coverage of 20% [37]. The rate of seasonal vaccine containing both H3N2 and pH1N12009 (v_{ab}) is set to ensure an annual coverage of 15% from 2010 onward, beginning in May for the Australian-like [24] and September for the UK-like scenarios. For simplicity we assume that vaccination rates are independent of immunological

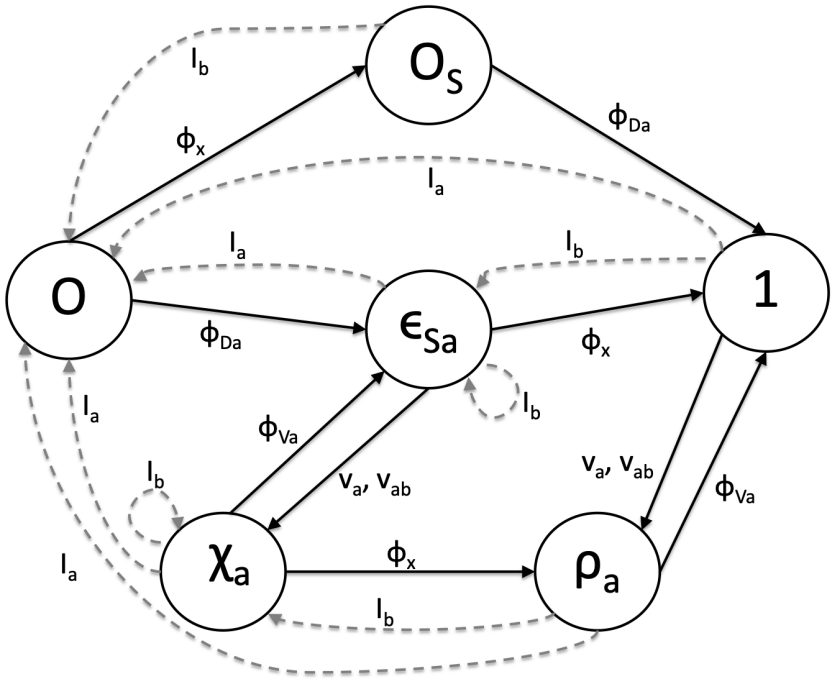

Figure 2: Model schematic indicating the types of susceptibility to subtype a: 1 indicates full susceptibility, ρ_a indicates vaccine-induced protection only, ϵ_{Sa} indicates heterologous cross-protection only, χ_a indicates vaccine-induced protection with heterologous cross-protection, 0 indicates infection-induced reduction in susceptibiity with heterologous cross-protection and 0_s indicates infection-induced reduction in susceptibility from infection without heterologous cross-protection. Directed lines indicate the mechanisms for transiting between different types of susceptible states. Dashed lines indicate changes driven by infection; I_a signals infection with strain a and I_b infection with strain b. Solid lines indicate changes driven by waning immunity and vaccination; ϕ_X indicates waning heterologous cross-protection, v_a (v_{ab}) signals vaccination against subtype a (a and b), Φ_{Va} signals waning vaccine protection and Φ_a signals waning NAb protection due to antigenic drift. Processes altering the susceptibility to subtype b are captured by the same flow diagram with $a \longleftrightarrow b$.

status, and hosts with remnant protection from a previous vaccination are re-vaccinated at the same rate as unvaccinated individuals. As pH1N12009 was not observed to drift sufficiently to warrant an update of the vaccine strain during the modelled period [87], we assume $\phi_{D,a} = 0$. For simplicity we optimistically assume $\rho_b = 0$.

2.2. Model calibration with Approximate Bayesian Computation

We denote by $\vec{\theta}$ the vector of transmission, pre-pandemic immunity, seasonal forcing and importation parameters required to simulate the model. We have motivated fixed values of some parameters in §2.1, but there are many remaining parameters which can be adjusted to calibrate the model. In a Bayesian context, the posterior $P(\vec{\theta}|D)$ encodes the information provided by data D about $\vec{\theta}$. ABC is a likelihood-free method to approximate $P(D|\vec{\theta})$ by defining a metric capturing the distance of the model output $D^* = D^*(\vec{\theta})$ from the data, $d(D, D^*)$, and exploiting the approximation $P(\vec{\theta}|D) \approx P(\vec{\theta}|d(D, D^*) \leq \epsilon)$ [see, e.g. 58]. Here we generate samples from the posterior using a 1-step rejection method, simulating from uniform priors for $\vec{\theta}$ using Latin Hypercube Sampling (LHS) [35] (see 2.2.1), and accepting $\vec{\theta}$ where $d(D, D^*) \leq \epsilon$. In §3 we present posterior predictive checks for the distance metric criteria, trajectory of infections and IARs.

2.2.1. Model priors

Priors for the initial conditions are chosen to be consistent with pre-pandemic serology for pH1N12009 in Australia and the UK, and are specified in Table B.1. Table B.2 summarises the priors on the transmission parameters, and we note a few key assumptions here. Pre-pandemic prevalence of serum antibody to seasonal H3N2 is allowed to vary widely. The prior for the phase offset θ_{offset} is chosen so that peak transmission occurs within a two month window centred around the beginning of July (January) for the Southern (Northern) hemisphere simulations. We sample across the full range of possibilities forρ_{pH1N1} and ρ_{H3N2}. Cross-protective immunity is assumed to be of low to moderate strength, $\epsilon_I \sim U(0.5, 1)$.

2.2.2. Distance metric

We construct d based on 12 hemisphere-dependent criteria (C_1–C_{12}) that we wish our model output to satisfy, which are described in Table 1. Here Years 1–5 refer to annual periods beginning in April 2009–April 2013 respectively and IARs are calculated from the cumulative incidence for the entire year (thus including any inter-seasonal activity). To summarise, criteria C_1 & C_3 require annual epidemics in the simulation dynamics with appropriate IARs guided by the rise of seroprevalence of pH1N1 antibody from serological surveys. Criterion C_9 refers to the seroprevalence to the pH1N12009 in the second year of its circulation (note the slightly different constraints for Australia and the UK). Criterion C_2 refers to the distinct second peak of pH1N12009 infection in Year 2. Criteria C_4–C_8 are based on the numbers of sub-typed isolates in sentinel and/or WHO influenza surveillance laboratories in Australia and equivalent reports from the UK. Criteria C_3 and C_9 are motivated by results from cross-sectional serological surveys. Criteria C_{10} and C_{12} reflect evidence for the prevalence cross-protection to both seasonal and pandemic subtypes that reduces host infectiousness. Criterion C_{11} refers to a double peaked pH1N1 epidemic in Year 1 and is only applied to the UK-like scenario.

Simulations are performed independently for each location and each parameter set, adjusting only the parameters governing the region dependent timing of seasonal forcing and vaccination campaigns. For a given parameter set, Table 1 specifies 23 conditions that we would wish a simulation to satisfy across both hemispheres in our ABC process. We define the distance from the model to the data via a union metric [49] (for $n_c > 1$):

$$d(D, D^*) = \frac{1}{[(1 - \Pi_{j=1}^{n_{C_e}} \mathbb{I}(C_{e,j}))/n_c + \Pi_{j=1}^{n_{C_e}} \mathbb{I}(C_{e,j})] \sum_{l=1}^{2} \sum_{i=1}^{i=12} \mathbb{I}(C_i^l)}, \tag{1}$$

where l indexes the locations considered (Australia, UK) and i indexes the criteria. We explore the sensitivity of our results to assuming that a vector of location dependent criteria $\vec{C}_e$, with length n_{C_e}, are essential, by including the first factor in the denominator of equation (1). We accept parameter sets $\vec{\theta}$ with $d(D, D^*) \leqslant \epsilon = \frac{1}{n_c}$ with $n_c = 19$. We trial two choices for $\vec{C}_e$. We firstly consider $\vec{C}_e = (C_{11}^2)$ as without satisfying C_{11} we do not select parameter sets displaying the double peaked incidence of pH1N1 in 2009 observed in the UK-like scenario. We also explore candidates with $\vec{C}_e = (C_{12}^1, C_{12}^2)$, ensuring an epidemiologically motivated minimal prevalence of cross-reactive, partial protection against transmission following a natural infection in both locations, the inclusion of which is a distinguishing feature of our model.

	Criteria	Reference
C_1	At least 4 epidemic peaks in each subtype over Years 1–5	Annual or near-annual circulation of each subtype
C_2	Peak incidence of pH1N1 in Year 2 at least 10% first peak	[86]
C_3	pH1N12009 IAR during Year 1 in the range 5-20%	[26, 53, 54, 56]
C_4	H3N2 IAR less than pH1N12009 IAR for Year 1	[50]
C_5	Australia: Total IAR for H3N2 and pH1N12009 in Years 2 and 3 lower than for Year 1 UK: Total IAR for H3N2 and pH1N12009 in Year 3 lower than for Year 1	[4] [32]
C_6	H3N2 IAR less than pH1N12009 IAR in Year 2	[14, 32]
C_7	Australia: H3N2 IAR less than 110% of pH1N12009 IAR in Year 3 UK : H3N2 IAR greater than pH1N12009 IAR in Year 3	[15] [32]
C_8	H3N2 IAR in Year 4 less than than pH1N12009 IAR	[16, 22]
C_9	Australia: Peak cross-sectional sero-prevalence to pH1N12009 in Year 2 is 30–60% UK: Peak cross-sectional sero-prevalence to pH1N12009 in Year 2 is 30-70%	[54] [36]
C_{10}	Cross-sectional cross-protection to pH1N12009 at least 50% of the pre-pandemic level at end of Year 5	[31]
C_{11}	For the UK only: two peaks of pH1N12009 infection in Year 1, with approximately 8-26 weeks separation.	[42, 56]
C_{12}	Cross-protection to both subtypes is common: $P_{X_{H3N2}\|X_{pH1N1}} > 0.25$, at least 10% of hosts have cross protection to each subtype $[\min(P_{X_{pH1N1}}, P_{X_{H3N2}}) > 0.1]$, over 25% of hosts have cross-protection to at least one subtype $[\max(P_{X_{pH1N1}}, P_{X_{H3N2}}) > 0.25)]$, and effective: $\epsilon_I < 0.7$.	[31]

Table 1: LHS filtering criteria. Note that some criteria differ slightly for simulations in the UK and Australia depending on surveillance data.

3. Results

3.1. ABC acceptance rates

Out of 100,000 LHS samples $\approx 0.0083\%$ satisfy threshold distance d: 69 of the candidates satisfy at least 19 criteria including C_{11} (henceforth Group 1) and 71 of the candidates satisfy this nominal threshold including C_{12} (henceforth Group 2). The distribution of the number of criteria satisfied in each hemisphere is shown in Figure B.1. The criterion that is least frequently satisfied

differs between the UK and Australian-like scenarios (see Figure B.1). For the UK-like scenarios the relative dominance of H3N2 and pH1N1 in Year 3 (C_7) is least frequently replicated in Groups 1 & 2. For the Australian-like scenarios the weak conservation of cross-protection (C_{10}) is satisfied least frequently amongst candidates in Groups 1 & 2.

Group	Requirements	No.
1	$d \leq 1/19$, $\vec{C_e} = (C^2_{11})$	69
2	$d \leq 1/19$, $\vec{C_e} = (C^1_{12}, C^2_{12})$	71
3	$d \leq 1/19$, $\vec{C_e} = (C^2_{11}, C^1_{12}, C^2_{12})$	58
4	$d \leq 1/19$, $\vec{C_e} = (C^2_{11}, C^1_{12}, C^2_{12})$, $\rho_{pH1N12009} \leq 0.5$	20

Table 2: Metric requirements for each group filtered from LHS and number of candidates satisfying each.

3.2. Candidate parameters

We present the marginal posterior median and range across posterior samples in each group in Tables C.1 & C.2.

The median basic reproduction number, $\mathcal{R}_0$ is approximately 1.26 for Group 1, and 1.29 for Group 2. The effective reproductive number $\mathcal{R}_e$ typically peaks at lower values often close to unity (Figure 3i&j), due to the immunity in the modelled populations. Other estimates of $\mathcal{R}_e$ from seroprevalence data are sensitive to the inclusion of children in serological surveys, and are as low as $\mathcal{R}_e \approx 1.14$ when excluding children [28]. The median amplitude of the seasonal forcing corresponds to increases in transmission by 6–7 per cent from the average for each subtype, but ranging from 1 per cent up to 10 per cent, roughly consistent with other estimates of variation due to climatic factors [78]. Posterior samples for the phase of seasonal forcing θ_{offset} take values across the prior within each group, however the prior is fairly narrowly constrained (see Table B.2). The median value for the H3N2 drift-rate ϕ_{H3N2} which would mimic antigenic replacement over approximately 3 years which is consistent with rates from phylogenetic analyses of this subtype [12]. The rate of loss of vaccine induced protection ϕ_v in posterior samples can vary with subtype but is always lost on a time-scale of less than one year, consistent with estimates from vaccine efficacy studies [64].

Hosts with cross-protection experience a median of approximately 40% reduction in infectiousness across posterior samples of ϵ_I, but candidate values of ϵ_I consistent with a limited effect of cross-protection on transmission exist in Groups 1 & 2. The median prevalence of pre-pandemic cross-protection to pH1N12009 ($P_{X_{pH1N1}}$) is 22% (23%) in Group 1 (2) and for H3N2 ($P_{X_{H2N2}}$) is approximately 40% for both groups. The overlap of hosts with cross-protection to both strains ($P_{X_{H3N2}|X_{pH1N1}}$) has posterior median 40% in Group 1 and slightly higher in Group 2 (46%) (as expected given the essential criteria imposed when selecting these candidates). The median proportion with neutralising protection against H3N2 (P_{H3N2}) is approximately a quarter, while (consistent with our tight sampling constraints) the proportion with neutralising immunity to pH1N1 is between 5 and 9 per cent. A non-negligible fraction ($P_{v_{H3N2}}$), 5–15%, are vaccinated against H3N2 at the beginning of the pandemic in our Group 1 and 2 candidates. Correlations between sampled parameters are presented in Figures C.1 & C.2.

There is a large common membership between Groups 1 and 2, which is reflected in the similarity of the range and median of the candidate parameters. In Section 3.3 we consider the 58 candidates who are members of both Groups 1 & 2 (denoted Group 3).

The efficacy of pH1N1 vaccination ρ_{pH1N1} varies widely across simulations suggesting that an efficacious vaccine is not required for our model to satisfy our union metric distance threshold.

Many of the Group 3 candidates have ρ_{pH1N1} corresponding to poor efficacy (defined here as $\rho_{pH1N1} \geq 0.5$). For the purpose of exploring the impact of pandemic vaccination in Section 3.4, we focus on the 20 candidates with $\rho_a < 0.5$, henceforth Group 4.

3.3. Capturing pH1N1 and seasonal H3N2 transmission dynamics

The posterior predictive check for Group 3 candidate dynamics is provided in Figure 3. The simulated Year 1 epidemic for the UK-like scenario has extended duration with higher inter-season levels of infection compared to the Australian-like scenario (Figure 3a&b). Model pH1N12009 IARs are highest in the year following pandemic onset (Year 1), and greater in the Australian-like scenario than the UK-like scenario (Figure 4). This is also true of posterior counterfactual simulations without vaccination (Figures C.23-C.24). Attack rates for pH1N12009 in subsequent years are smaller, and the Year 2 pH1N12009 IAR is weakly inversely correlated with the Year 1 pH1N12009 IAR. Our filtering criteria do not select for the timing or shape of epidemics within each annual period, and therefore epidemics in each hemisphere tend to begin when the simulations begin, earlier than the June/July first wave observed in the UK.

Most Group 3 candidates recover the sharp rise in seroprevalence of sterilising antibody to pH1N12009 following the pandemic wave and subsequent vaccination campaign (C_9) in the Australian-like scenario. The corresponding sero-prevalence to pH1N12009 rises more gradually in the UK-like scenario, but plateaus at a similar level following Year 2 (Figure 3c&d). The peaks and troughs superimposed on this trend are due to the acquisition and loss of vaccine acquired protection (since $\phi_{D,pH1N12009} = 0$ in our model). Consistent with the imposed filtering (C_{10}, C_{12}) approximately 10–20 per cent of hosts initially have cross-protection to both circulating subtypes. The prevalence of hosts with cross-protection to either subtype tends to fall during the simulations, though is transiently sustained or boosted by the large initial pandemic wave (Figure 3e,f,g&h). The time-dependent local effective reproduction number in Figure3i&j accounts for the shifting population immune profile, potential infectiousness and seasonality in transmissibility equation (A.3). Note that $\mathcal{R}_{\mathrm{e,i}}$ does not always peak above one during each annual period, indicating circulation is often sustained by importations in the model. Indeed $\mathcal{R}_0$ and c_{H2N2} are inversely correlated amongst Group 1 and 2 candidates (see Figure C.1). Local bivariate sensitivity analyses highlight the influence of the constant importation rate ($c_{pH1N12009}$) on the timing and size of the initial peaks of pH1N12009, with higher importation rates typically preferred (see Figures C.11-C.14, Appendix C.2.3). In contrast our model has limited sensitivity to the much smaller seasonal fluctuations (controlled by $s_{pH1N12009}$). Given estimates of the population size [3, 79] and the number of incoming domestic and international travellers in 2009 [2, 62], our maximum value of $c_{pH1N12009} = 10^{-4}$/capita/year indicates a modest average incoming prevalence of 0.018% for Australia and 0.0066% for the UK during 2009.

3.4. Seasonality, pandemic timing and vaccination impact

Without monovalent vaccination against pH1N12009 in Year 1, Group 4 simulations yield a Year 1 pH1N12009 IAR which is $\approx 17 - 36\%$ in the Australian-like scenario and $\approx 17 - 30\%$ in the UK-like scenario (Figures C.23-C.24). Simulations with the default vaccination campaign yield a reduction in the Year 1 pH1N12009 IAR (ΔIAR) of less than 1 percentage point in the Australian-like scenario but $\approx 1 - 10$ percentage points in the UK-like scenario (Figure C.22). For the UK-like simulations, all but one of the Group 4 candidates suggests pandemic vaccination campaigns reduced the Year 1 pH1N12009 IAR by $\Delta\mathrm{IAR} \geq 1.5$ percentage points. A lone Group 4 candidate with $\Delta\mathrm{IAR} < 1$ has a very high baseline Year 1 pH1N12009 IAR of $\approx 30\%$ (Figure C.22).

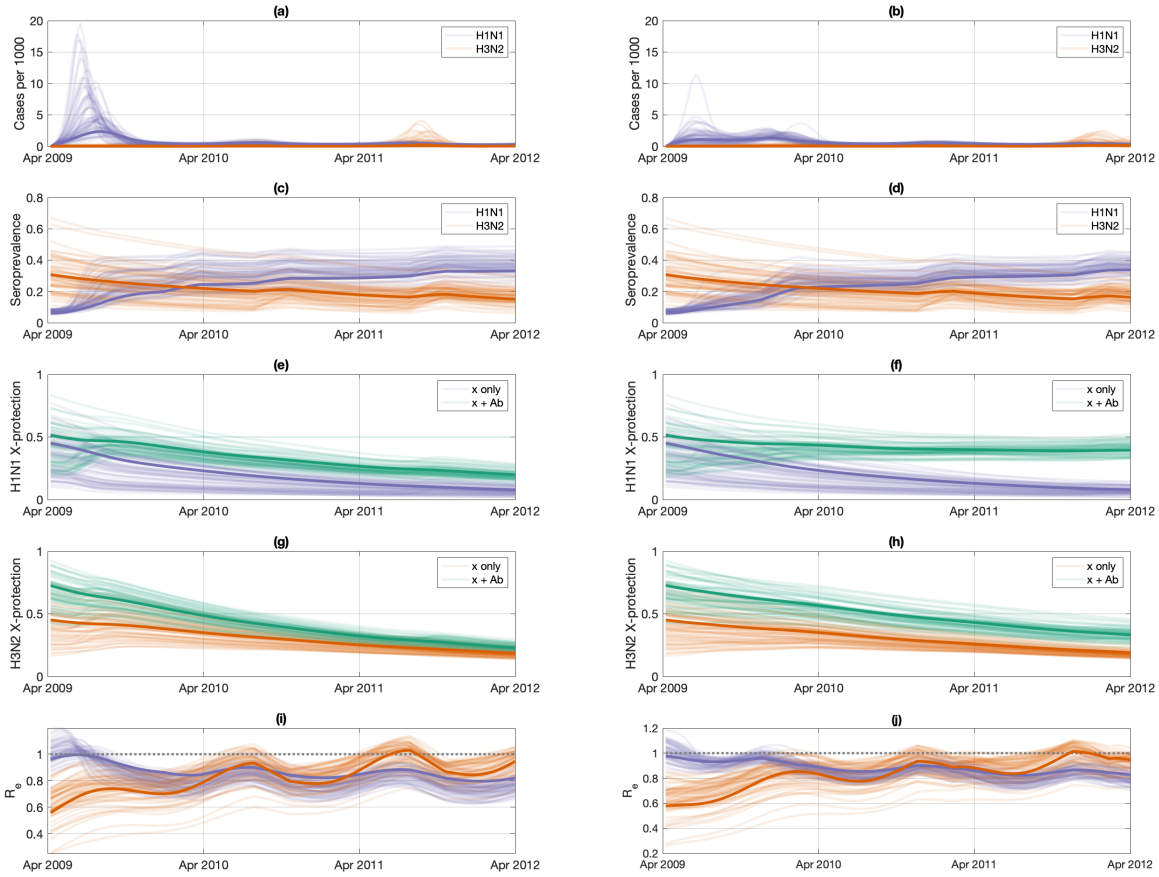

Figure 3: *Left*: Australian-like scenario for Group 3 candidates. *Right*: UK-like scenario for the same candidates. **(a) & (b)**: incidence of infection per 1000 population with pH1N1 (purple) and H3N2 (orange) curves, **(c) & (d)**: the proportion of the population sero-protection assuming immediate protection following infection or vaccination to pH1N1 (purple) and H3N2 (orange), **(e) & (f)**: proportion of the population with only cross-protection to against H1N1 (purple) or with cross-protection and infection induced antibodies (turquoise), **(g) & (h)**: proportion with only cross-protection against H3N2 (orange) or cross-protection with infection induced antibodies (turquoise), **(i) & (j)**: effective reproduction number for pH1N12009 (purple) and H3N2 (orange). One of the several candidates with the smallest realised value of $d(D, D^*)$ [equation (1)] is sketched in bold.

Motivated by the contrast between the impact of very similar pandemic vaccination campaigns in the UK-like and Australian-like scenarios, we perform a sensitivity analysis for our Group 4 candidates on the potential benefit of vaccination campaigns across all possible offsets between IAV seasonality and pandemic emergence (controlled by ϕ_{offset}). We compare default vaccination campaigns to counterfactual vaccination campaigns with the same coverage that are delivered 3 months earlier than was achieved ('early') or with the same timing but with a perfectly efficacious vaccine ('perfect').

We note that baseline modelled pH1N12009 Year 1 IAR are seasonal and lowest when seasonal forcing peaks ≈ 11 months after pandemic onset. The seasonality in IAR is preserved when considering the first two years of pandemic IAV circulation (Figure C.19). The averted infections in the presence of vaccination campaigns are also seasonal, although the timing of averted infections

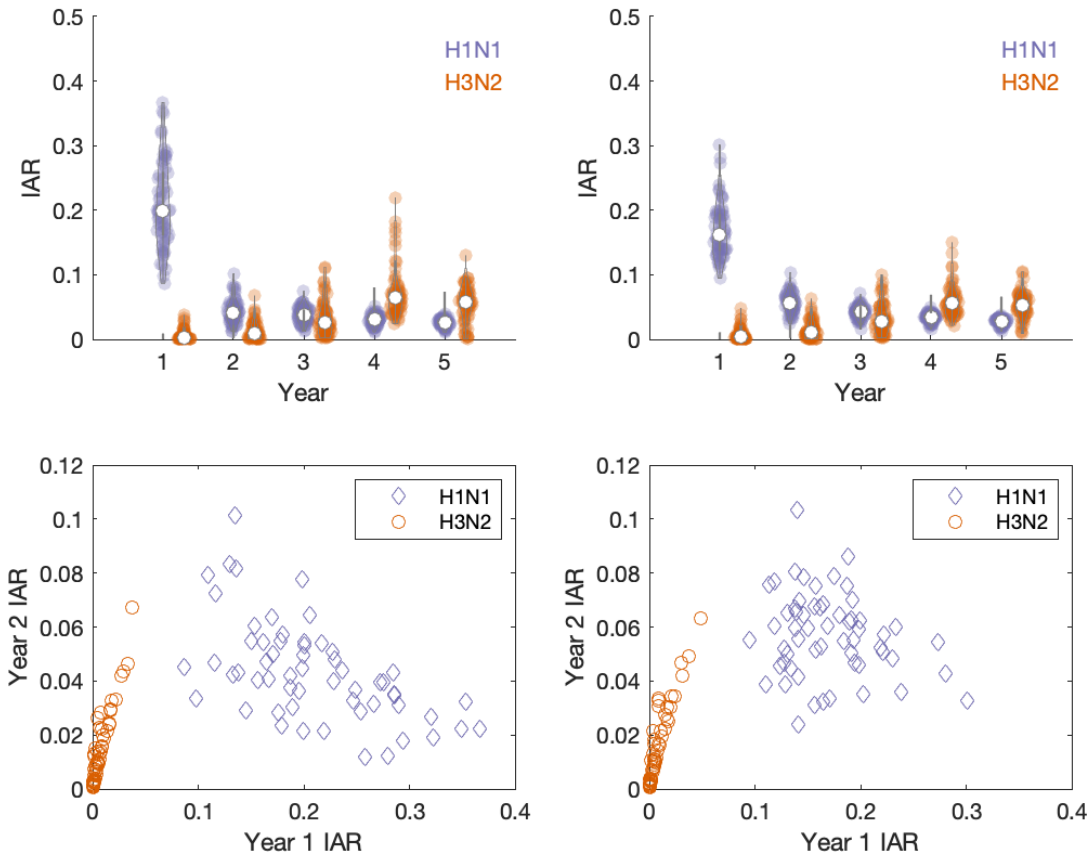

Figure 4: *Upper panels:* Annual attack rate for Group 3 candidates in Australian-like scenarios (left) and UK-like scenarios (right). White circles indicate the median in Group 3. *Lower panels:* Attack rates in Years 1 and 2 for pH1N12009 (purple diamonds) and H3N2 (orange circles).

differs with the nature of the modelled vaccination campaign and the time-frame considered (Figure 5). When considering the Year 1 pH1N12009 IAR only, early vaccination campaigns are most effective at reducing the IAR, and this benefit is maximal when seasonal forcing peaks ≈ 9 months after pandemic onset. Perfect and default counterfactual vaccination simulations have maximal impact when the seasonal forcing peaks ≈ 10 months after pandemic offset. For many Group 4 candidates and seasonal offsets even vaccination campaigns up to 12 weeks earlier than achieved in 2009 cannot significantly reduce the Year 1 pH1N12009 IAR over a large range of timings for the emergence of sustained pandemic virus transmission with respect to seasonal influenza. When considering the summed Year 1 and 2 pH1N12009 IAR perfect and early vaccination campaigns have similar maximal impact. However early vaccination campaigns have higher median reduction in IAR than perfect campaigns when seasonal forcing peaks 6–9 months after vaccine offset, whereas perfect vaccination campaigns have higher median impact when this offset is 10–12 or 1–2 months.

Posterior samples can be influenced by the choice of ρ_{H3N2} (Figures C.6-C.6, Appendix C.2.1), however trends in the pH1N12009 IAR with the timing of seasonal forcing are insensitive to the strong assumptions regarding seasonal vaccine efficacy for Group 4 candidates (Figure C.20) and we expect our main conclusions to hold despite our simplifying assumption $\rho_{\mathrm{H3N2}} = 0$. The combined

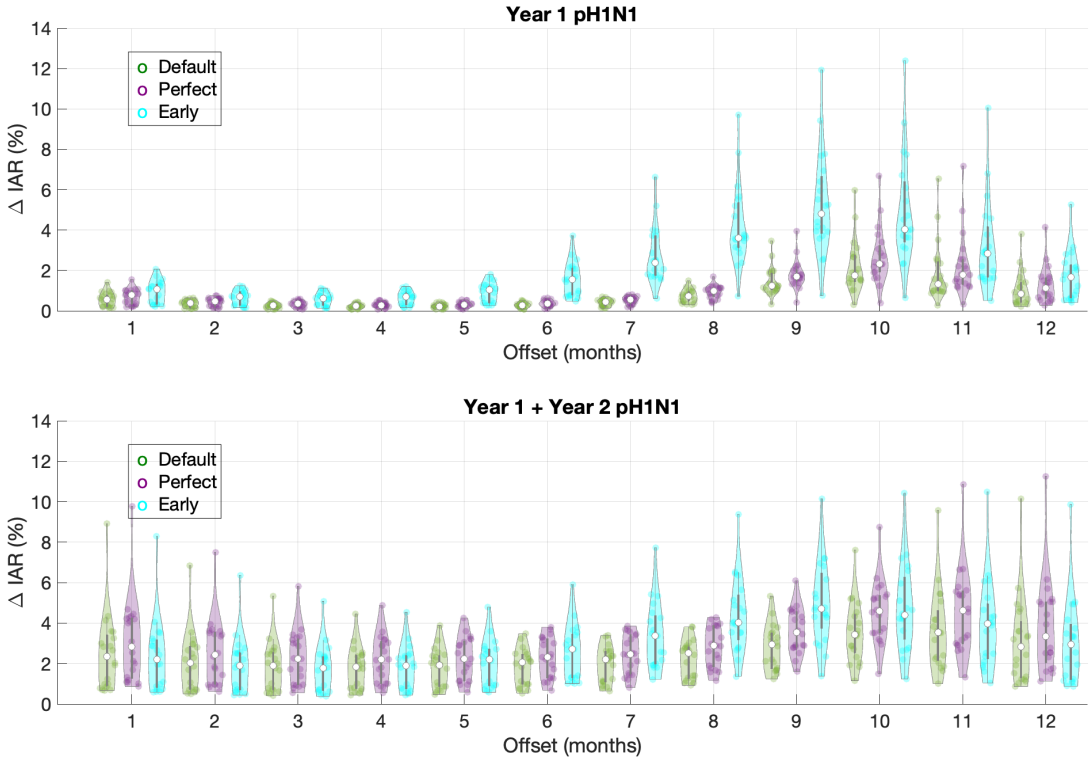

Figure 5: Reduction of pH1N12009 Year 1 IAR under default vaccination for Group 4 candidates (green), or with a perfect vaccine and coverage with the same timing (purple), or the same efficacy but 12 week earlier outroll (cyan). Lower panels show the cumulative reduction in pH1N12009 IARs for Year 1 and Year2. Offset indicates the time between pandemic onset and peak seasonal forcing (as in Figure **??**).

.

benefit of early and perfect vaccination against pH1N12009 is explored further in Figures C.21 & C.22.

We also explore the implications of very high vaccination coverage and find that even 90% vaccine coverage does not alter the burden of pH1N12009 infection in the Australian-like Southern Hemisphere scenario on short time-scales (Figure C.24), but there is still a small cumulative benefit over 5 years that is slightly enhanced in the UK-like scenario (Figures C.23 & C.24).

3.5. Role of cross-protection in model dynamics

Heterosubtypic immunity of intermediate duration that reduces onward transmission but not susceptibility is well motivated by animal and human studies, yet typically neglected in $SIRS$-type transmission models for IAV. We consider a bi-variate sensitivity analysis amongst Group 4 candidates, considering the influence of ϵ_I and ρ_{pH1N1} on IAV and d (with $\vec{C}_e = (C_{11}^2, C_{12}^1, C_{12}^2)$). Although the inclusion of C_{12} in $\vec{C}_e$ preferences values of $\epsilon_I < 0.7$, parameter combinations satisfying C_{12} often have values closer to the minimum sampled value of $\epsilon_I = 0.5$ (left panels, Figures C.7-C.10). Year 1 and 2 pH1N12009 IARs are very sensitive to ϵ_I (Figures C.7-C10), more so than than the pandemic vaccine efficacy ρ_{pH1N1}: increasing ϵ_I from 0.5 to 1 can increase the Year 1 pH1N12009 IAR by over 10 percentage points, while changing vaccine efficacy between its limits has minimal effect (middle panels, Figures C.7-C.10, Appendix C.2.4). The magnitude of this effect varies between Group 4 candidates, but the trend is consistent, and likely explained by the

presence of cross-protection at pandemic onset and with greater longevity than vaccine induced immunity in our model. Indeed we find a significant negative correlation of moderate strength in selected values of $\mathcal{R}_0$ and $P_{X_{pH1N1}}$ (Figure C.1). Amongst Group 4 candidates $\approx 14-66\%$ (median 29%) of hosts have some cross-protection to the pandemic strain at pandemic onset. The burden of infection due to the non-pandemic IAV virus (H3N2) is not, however, impacted by high levels of coverage with a monovalent pH1N12009 vaccine (Figures C.23-C.24), even though this could preclude generation of cross-protection in this cohort, likely reflecting the short duration of vaccine induced immunity in selected candidates.

3.6. Impact of school holidays on model dynamics in the UK

Group 3 candidates often show two peaks of infection in the spring/summer of 2009 for the UK-like scenarios, with another small wave in the 2009–2010 influenza season. The shape of these waves of infection, however, do not accurately reflect that observed in Northern Hemisphere countries. Figure 1 shows that the first and second waves of infection are separated by a distinct trough in the number of specimens detected, whereas, the two waves of infection in our candidate parameter sets are separated by a very shallow trough. When school closure is included in the model (with overall mixing reduced by a factor $\sim U(0, 0.5)$ during end of term breaks and by a factor $\sim U(0.7, 1)$ during mid-term breaks, appropriate for various countries in the Northern Hemisphere) Group 3 parameter sets show qualitatively similar dynamics to that shown in Figure 1. When school closure is included in the simulation the magnitude of the 2010–2011 wave (Year 2 pH1N12009 IAR) increased (see **??**). However only a single Group 3 candidate with school closure has pH1N12009 IARs exceeding 10% in Year 1 and Year 2 (Figure C.27).

4. Discussion

We introduced a model for the co-circulation of two influenza subtypes to explore the influence of the timing and efficacy of vaccination campaigns on the dynamics of pH1N12009 infection in the presence of a seasonal H3N2 subtype. We show that in an Australian-like scenario, where the pH1N12009 began community transmission only a month or two prior to the usual seasonal influenza season, the first wave of the pandemic was more likely to be rapid with a high pH1N12009 IAR over 20%. In this situation, earlier vaccination campaigns can induce reductions in the Year 1 pH1N12009 IAR of less than approximately 2 percentage points, even when vaccines are perfectly efficacious and delivery begins three months earlier than was achieved. This is consistent with seroepidemiology suggesting that Year 1 infection plus vaccination was able to largely suppress further transmission in Year 2 in the Australian-like scenario [53]. In our simulations mimicking an equivalent UK-like scenario, vaccination campaigns that begin approximately 6 months after introduction of the pandemic virus are more effective at reducing the pH1N12009 IAR for the first two years of pandemic spread. This enhanced impact is driven by the longer, often double-peaked, epidemic in the first year of pandemic transmission when pandemic emergence is out of season. For simulations in both hemispheres, where vaccination is able to reduce the modelled Year 1 pH1N12009 IAR, this is correlated with a larger Year 2 IAR. These results reinforce the benefit of responding early in a pandemic with a 'universal' vaccine that can trigger or boost influenza-specific cytotoxic T cells [8] to further limit transmission from hosts infected with a novel IAV strain for the IAR. In concluding this we have only considered the impact of immune protection against infection and transmission on overall IARs; enhanced heterologous immune responses due to infection and/or vaccination may yield more durable protection against severe disease, as observed in some studies of SARS-CoV-2 vaccine immunogenicity and efficacy [71, 88].

We have also not considered other relevant measures of epidemic severity such as peak incidence and epidemic duration.

A univariate sensitivity analysis of the role of the phase of seasonal forcing in our model suggests there is a strong signature of influenza seasonality in the expected impact of any pandemic vaccination campaign, that is magnified in delayed campaigns. Towers *et al.* use an SIR model with harmonic seasonality and a simple age-structure to demonstrate that the benefits of school closure in a pandemic scenario depend on seasonal factors influencing transmissibility [75]. Lee & Chowell also use an SIR model to explore the impact of the timing of epidemic emergence with respect to seasonality and the timing of vaccination (and treatment), reporting that delayed vaccination results in poorer outcomes when $\mathcal{R}_0 < 2$ [45]. A modelling study of global pandemic influenza circulation with top-hat seasonal forcing and air-travel motivated choices for importations yields similar conclusions regarding the poor efficacy of vaccination campaigns in southern temperate regions [39]. Our study adds to this work by considering multi-dimensional immunity and the medium-term impact of pandemic vaccination on subsequent IAV seasons.

We have preferentially selected (through inclusion of C_{12} in $\vec{C}_e$) models with a minimal prevalence of cross-protective immunity against infectiousness in our model. We have enforced loss of this cross-protective immunity after an average of 2 years. With these constraints it is often difficult to have weak conservation of cross-protection (reflected in low rates of the criterion C_{10} being satisfied). However declining population-levels of influenza specific cytotoxic T cells may be expected following an IAV pandemic due the prevalence of recently acquired immunity, and such a trend was noted in the 5 years following the 1977 pandemic [52]. Models in which cross-protection wanes more gradually would further suppress seasonal IAV in our model. Other computational modelling studies have suggested that partially protective immunity of intermediate duration is parsimonious with the epidemiological and evolutionary characterisations of influenza [23]. Truscott *et al.* [77] also report that cross-protection is required to explain multistrain IAV dynamics, however in that model cross-protection is assumed to reduce susceptibility rather than infection and wane in synchrony with strain-specific immunity. If the invoked cross-protective immunity in our modelling reflects its contribution to reducing transmission in a typical influenza season, the dearth of circulation of IAV over the 2 years since NPIs were introduced in response to SARS-CoV-2 [44], could result in significantly reduced protection that could translate to higher than usual reproduction rates for the same social contact patterns (see also [33] for a modelling study predicting resurgence in the rates of severe IAV infection).

The UK experienced a large third wave of pH1N12009 in the 2010-2011 influenza season [86], not reproduced in our study even when we include reductions in the contact rate during school holiday periods. A direct conclusion of this result is that the inclusion of age structure in our model may allow a study of this large third wave phenomenon, with the caveat that we have made very simple assumptions about the impact of school holidays on overall transmission rates [20, 21], but in practice the impact of holidays will depend on the age-dependent epidemic progression, the employment status of parents of school aged children, and the social activity connecting pupils and their community during the holidays [e.g. 27]. Differences in age-dependent assortative mixing, pre-existing immune profiles and demographics may also be at play [48]; several longitudinal cross-sectional sero-prevalence studies suggest that early attack rates were higher in school aged children [19], with incidence in successive waves shifting into older age-groups [36, 53]. The efficacy of seasonal influenza vaccination can vary by year and age group [46]. However, an analysis of pH1N12009 in the UK using an age-structured transmission model, and allowing for some changes in case ascertainment, found that the third wave could not be replicated using age groups and school closure alone, but required an increase in pH1N12009 transmission in the 2010-2011 influenza

season [18], highlighting the challenges of explaining medium-term trends in IAV circulation.

Our assumptions of similar pre-pandemic immunological conditions across hemispheres neglects differences in short-lived heterosubtypic immunity related to the timing of previous epidemics that may drive seasonality in the possible timings of pandemic emergence [25]. It is possible that any such effect is absorbed into our estimated seasonal forcing. Further exploration of the role of cross-protective immunity as distinct from other types of immunity and seasonal drivers in modelling studies is warranted to understand its role in shaping IAV epidemiology. Given the widespread prevalence of cross-protective CD8+ T-cells [31], which may not be explained purely by effector CD8+ T-cells, characterising this response may require decoupling memory and effector CD8+ T cells in our model. Within-host modelling of IAV infections incorporating cellular and humoral responses which can differentiate the impact of CTL pool size on viral clearance could be used to motivate different population-level characterisation of the infection history driven multi-factorial host immune state [11]. Indications that inactivated virus influenza vaccines can induce influenza T-cells [66], and age-dependence of waning vaccine-induced immunity [64], may also be relevant for future modelling of the impact of pandemic vaccination campaigns. Differences in national IAV vaccination policies, particularly around use of live attenuated IAV vaccines (which can induce cellular responses in children [81], and are currently used in paediatric populations in the UK [61] but not Australia [13]) could lead to global divergence in population immune profile that may drive differences in outcomes of future IAV pandemics and associated interventions.

Our approach has a number of additional limitations. Using a simple ABC approach, we selected model parameter sets that satisfied a threshold number of epidemiological constraints but have not obtained formal fits to the data through dense sampling of the posterior and adjustment of the tolerance, as in, for example, ABC-SMC [58]. Although our model includes many possible immunological states, it is simple in its assumption of homogeneous mixing, age-independent vaccination and immunity, and exponentially distributed waiting times between model states. The failure of our model to concurrently satisfy all defined criteria highlights the limitations of our model to capture epidemiological characteristics in multiple locations. Modelling the seasonal forcing in each location based on regional meteorological/social mixing considerations may ease this discrepancy. Accounting for differences in travel patterns between countries may be more appropriate than the fixed per-capita importation parameter adopted here [e.g. 39]. We have not modelled case ascertainment which could change over time driving, for example, apparent troughs in case time series.

Importantly, our conclusions relate only to pandemic scenarios in which the emerging subtype has a history of circulation in humans ($P_a > 0$), that both constrains its initial spread and the evolutionary scope for rapid changes in antigenicity (i.e. we set $\phi_{pH1N1} = 0$ over our 5 year simulations) or virulence (i.e. we fix the intrinsic maximal transmissibility $\mathcal{R}_0$) [73]. Our conclusions would likely be less relevant for pandemics triggered by viruses with a limited history of circulation in humans that may be expected to generate a large epidemic regardless of seasonal factors, and may be followed by rapid adaptation to the human population that could generate multiple severe waves of infection [9, 38, 45].

5. Conclusions

Our analysis suggests that the small post-pandemic waves of pH1N12009 infection in Australia arose because the initial pandemic wave was enhanced by seasonal forcing, driving rapid depletion of the susceptible pool that left fewer hosts to fuel further waves of infection, rather than because the adopted vaccine was particularly efficacious or had a well-timed distribution. Although the

timing of a vaccination campaign can have a small impact on the cumulative infections over the first years of the pandemic, the potential benefit is inversely related to the size of the initial wave, highlighting the inadequacy of the current pandemic influenza vaccination strategies. In pandemics with low reproduction numbers, strategies for vaccine outroll might prioritise regions in which the pandemic is emerging in synchrony with seasonal outbreaks. However, if vaccine availability is delayed similarly to in 2009, the biggest gains may be in distributing to regions for whom the pandemic transmission has yet to experience seasonal enhancement.

Robust predictions of the role of seasonality on the potential impact of interventions such as vaccination will require more detailed modelling of the influence of meteorological and environmental factors on transmission, mixing behaviour and immune response [74]. Predictions for the timing of an outbreak in a given region may remain elusive given the dependence on importations via travel, uncertainty in local climatic conditions, and stochastic effects [59]. However, the insight that earlier vaccination campaigns make curbing the attack rate for the initial wave of pandemic influenza possible over a wider range of scenarios for seasonal forcing is likely to remain for low to intermediate values of $\mathcal{R}_0$ [45]. Extending modelling to incorporate within-host immunological dynamics, time-varying transmissibility and importation to tropical and sub-tropical regions where the seasonal drivers of transmission are less well understood could help inform global influenza control strategies.

Funding

KJB acknowledges support from a University of Melbourne McKenzie Fellowship and a University of Nottingham Anne McLaren Fellowship.

CRediT authorship contribution statement

KJB: Conceptualisation, Methodology, Software, Investigation, Formal analysis, Writing - Original Draft, Writing - Review & Editing, Visualisation. **JMMcC:** Conceptualisation, Methodology, Writing - Review & Editing, Supervision. **MPD:** Software, Methodology, Investigation, Writing - Review & Editing. **JMcV:** Conceptualisation, Writing – Review & Editing, Supervision. **JMH:** Conceptualisation, Methodology, Software, Formal analysis, Investigation, Writing - Original draft, Writing - Review & Editing, Visualisation, Supervision.

References

[1] Andrews, N., Waight, P., Yung, C.F., Miller, E., 2011. Age-specific effectiveness of an oil-in-water adjuvanted pandemic (H1N1) 2009 vaccine against confirmed infection in high risk groups in England. Journal of Infectious Diseases 203, 32–39.

[2] Australian Bureau of Statistics, a. Overseas arrivals and departures, australia, dec 2009.

[3] Australian Bureau of Statistics, b. Population by age and sex, regions of australia, 2009.

[4] Australian Government Department of Health and Aging, 2013. Australian Influenza Surveillance Report No. 6, 2013.

[5] Baker, M., Kelly, H., Wilson, N., 2009. Pandemic H1N1 influenza lessons from the southern hemisphere. Eurosurveillance 14, 19370.

[6] Bandaranayake, D., Huang, Q.S., Bissielo, A., Wood, T., Mackereth, G., Baker, M.G., Beasley, R., Reid, S., Roberts, S., Hope, V., et al., 2010. Risk factors and immunity in a nationally representative population following the 2009 influenza A (H1N1) pandemic. PloS one 5, e13211.

[7] Bishop, J.F., Murnane, M.P., Owen, R., 2009. Australia's winter with the 2009 pandemic influenza A (H1N1) virus. New England Journal of Medicine 361, 2591–2594.

[8] Bolton, K.J., McCaw, J.M., Brown, L., Jackson, D., Kedzierska, K., McVernon, J., 2015. Prior population immunity reduces the expected impact of CTL-inducing vaccines for pandemic influenza control. PLoS One 10, e0120138.

[9] Bolton, K.J., McCaw, J.M., McVernon, J., Mathews, J.D., 2014. The influence of changing host immunity on 1918–19 pandemic dynamics. Epidemics 8, 18–27.

[10] Broberg, E., Nicoll, A., Amato-Gauci, A., 2011. Seroprevalence to influenza A (H1N1) 2009 virus—where are we? Clinical and vaccine immunology: CVI 18, 1205.

[11] Cao, P., Wang, Z., Yan, A.W., McVernon, J., Xu, J., Heffernan, J.M., Kedzierska, K., McCaw, J.M., 2016. On the role of CD8+ T cells in determining recovery time from influenza virus infection. Frontiers in immunology 7, 611.

[12] Cox, N.J., Subbarao, K., 2000. Global epidemiology of influenza: past and present. Annual review of medicine 51, 407–421.

[13] Department of Health and Aged Care, Australian Government, 2022. Australian Immunisation Handbook. Accessed 7/2/23.

[14] Department of Health and Aging, Australian Government, 2010. Australian Influenza Surveillance report, No 44 2010.

[15] Department of Health and Aging, Australian Government, 2011. Australian Influenza Surveillance Report, No15 2011.

[16] Department of Health and Aging, Australian Government, 2012. Australian Influenza Surveillance Report, No 10 2012.

[17] Doherty, P.C., Turner, S.J., Webby, R.G., Thomas, P.G., 2006. Influenza and the challenge for immunology. Nature immunology 7, 449–455.

[18] Dorigatti, I., Cauchemez, S., Ferguson, N.M., 2013. Increased transmissibility explains the third wave of infection by the 2009 H1N1 pandemic virus in England. Proceedings of the National Academy of Sciences 110, 13422–13427.

[19] Dowse, G.K., Smith, D.W., Kelly, H., Barr, I., Laurie, K.L., Jones, A.R., Keil, A.D., Effler, P., 2011. Incidence of pandemic (H1N1) 2009 influenza infection in children and pregnant women during the 2009 influenza season in Western Australia—a seroprevalence study. Medical Journal of Australia 194, 68–72.

[20] Eales, O., Wang, H., Haw, D., Ainslie, K.E., Walters, C.E., Atchison, C., Cooke, G., Barclay, W., Ward, H., Darzi, A., et al., 2022. Trends in sars-cov-2 infection prevalence during england's roadmap out of lockdown, january to july 2021. PLOS Computational Biology 18, e1010724.

[21] Eames, K., 2014. The influence of school holiday timing on epidemic impact. Epidemiology & Infection 142, 1963–1971.

[22] England, P.H., 2014. Surveillance of influenza and other respiratory viruses in the United Kingdom: Winter 2013/14.

[23] Farrow, D.C., Burke, D.S., Rosenfeld, R., 2015. Computational Characterization of Transient Strain-Transcending Immunity against Influenza A. PloS one 10, e0125047.

[24] Fielding, J.E., Grant, K.A., Garcia, K., Kelly, H.A., . Effectiveness of seasonal influenza vaccine against pandemic (H1N1) 2009 virus, Australia, 2010 .

[25] Fox, S.J., Miller, J.C., Meyers, L.A., 2017. Seasonality in risk of pandemic influenza emergence. PLoS computational biology 13, e1005749.

[26] Gilbert, G.L., Cretikos, M.A., Hueston, L., Doukas, G., O'Toole, B., Dwyer, D.E., 2010. Influenza A (H1N1) 2009 antibodies in residents of New South Wales, Australia, after the first pandemic wave in the 2009 southern hemisphere winter. PLoS One 5, e12562.

[27] Glass, K., Barnes, B., 2007. How much would closing schools reduce transmission during an influenza pandemic? Epidemiology 18, 623–628.

[28] Glass, K., Kelly, H., Mercer, G.N., 2012. Pandemic influenza H1N1: reconciling serosurvey data with estimates of the reproduction number. Epidemiology , 86–94.

[29] Global Influenza Programme WEP, WHO, 2022. Assessment of risk associated with recent influenza A(H5N1) clade 2.3.4.4b viruses. Date accessed: 6/2/2023.

[30] Gog, J.R., 2008. The impact of evolutionary constraints on influenza dynamics. Vaccine 26, C15–C24.

[31] Hayward, A.C., Wang, L., Goonetilleke, N., Fragaszy, E.B., Bermingham, A., Copas, A., Dukes, O., Millett, E.R., Nazareth, I., Nguyen-Van-Tam, J.S., et al., 2015. Natural T cell–mediated protection against seasonal and pandemic influenza. Results of the flu watch cohort study. American journal of respiratory and critical care medicine 191, 1422–1431.

[32] Health Protection Agency, 2011. Surveillance of Influenza and other Respiratory Diseases in the UK, 2010/11.

[33] Hill, E.M., Keeling, M.J., 2022. Scenario modelling for diminished influenza seasons during 2020/2021 and 2021/2022 in england. medRxiv `https://www.medrxiv.org/content/early/2022/10/30/2022.10.27.22281628.full.pdf`.

[34] Hine, D., 2010. The 2009 Influenza Pandemic.

[35] Hoare, A., Regan, D.G., Wilson, D.P., 2008. Sampling and sensitivity analyses tools (SaSAT) for computational modelling. Theoretical Biology and Medical Modelling 5, 1–18.

[36] Hoschler, K., Thompson, C., Andrews, N., Galiano, M., Pebody, R., Ellis, J., Stanford, E., Baguelin, M., Miller, E., Zambon, M., 2012. Seroprevalence of influenza A (H1N1) pdm09 virus antibody, England, 2010 and 2011. Emerging infectious diseases 18, 1894.

[37] Institute of Health and Welfare, Australian Government, 2010. 2010 pandemic vaccination survey. Accessed December 2022.

[38] Jackson, C., Vynnycky, E., Mangtani, P., 2010. Estimates of the transmissibility of the 1968 (Hong Kong) influenza pandemic: evidence of increased transmissibility between successive waves. American journal of epidemiology 171, 465–478.

[39] Kenah, E., Chao, D.L., Matrajt, L., Halloran, M.E., Longini Jr, I.M., 2011. The global transmission and control of influenza. PloS one 6, e19515.

[40] Kobinger, G.P., Meunier, I., Patel, A., Pillet, S., Gren, J., Stebner, S., Leung, A., Neufeld, J.L., Kobasa, D., von Messling, V., 2010. Assessment of the efficacy of commercially available and candidate vaccines against a pandemic H1N1 2009 virus. The Journal of infectious diseases 201, 1000–1006.

[41] Krammer, F., 2020. SARS-CoV-2 vaccines in development. Nature 586, 516–527.

[42] Kubiak, R.J., McLean, A.R., 2012. Why was the 2009 influenza pandemic in England so small? PloS one 7, e30223.

[43] Lansbury, L.E., Smith, S., Beyer, W., Karamehic, E., Pasic-Juhas, E., Sikira, H., Mateus, A., Oshitani, H., Zhao, H., Beck, C.R., et al., 2017. Effectiveness of 2009 pandemic influenza A (H1N1) vaccines: A systematic review and meta-analysis. Vaccine 35, 1996–2006.

[44] Laurie, K.L., Rockman, S., 2021. Which influenza viruses will emerge following the sars-cov-2 pandemic? Influenza and other respiratory viruses 15, 573–576.

[45] Lee, S., Chowell, G., 2017. Exploring optimal control strategies in seasonally varying flu-like epidemics. Journal of theoretical biology 412, 36–47.

[46] Lewnard, J.A., Cobey, S., 2018. Immune history and influenza vaccine effectiveness. Vaccines 6, 28.

[47] Li, T., Fu, C., Di, B., Wu, J., Yang, Z., Wang, Y., Li, M., Lu, J., Chen, Y., Lu, E., et al., 2011. A two-year surveillance of 2009 pandemic influenza A (H1N1) in Guangzhou, China: from pandemic to seasonal influenza? PLoS One 6, e28027.

[48] Lugnér, A.K., van Boven, M., de Vries, R., Postma, M.J., Wallinga, J., 2012. Cost effectiveness of vaccination against pandemic influenza in European countries: mathematical modelling analysis. Bmj 345.

[49] McKinley, R., Hung, F., Wiest, R., Liebeskind, D.S., Scalzo, F., 2018. A machine learning approach to perfusion imaging with dynamic susceptibility contrast MR. Frontiers in neurology 9, 717.

[50] McLean, E., Pebody, R., 2010. Epidemiological report of pandemic (H1N1) 2009 in the UK, April 2009 – May 2010.

[51] McMichael, A., Dongworth, D., Gotch, F., Clark, A., Potter, C., 1983a. Declining T-cell immunity to influenza, 1977-82. The Lancet 322, 762–764.

[52] McMichael, A., Dongworth, D., Gotch, F., Clark, A., Potter, C., 1983b. Declining T-cell immunity to influenza, 1977-82. The Lancet 322, 762–764.

[53] McVernon, J., Laurie, K., Faddy, H., Irving, D., Nolan, T., Barr, I., Kelso, A., 2014. Seroprevalence of antibody to influenza A (H1N1) pdm09 attributed to vaccination or infection, before and after the second (2010) pandemic wave in A ustralia. Influenza and other respiratory viruses 8, 194–200.

[54] McVernon, J., Laurie, K., Nolan, T., Owen, R., Irving, D., Capper, H., Hyland, C., Faddy, H., Carolan, L., Barr, I., et al., 2010. Seroprevalence of 2009 pandemic influenza A (H1N1) virus in Australian blood donors, October–December 2009. Eurosurveillance 15, 19678.

[55] McVernon, J., Nolan, T., 2011. Panvax®: a monovalent inactivated unadjuvanted vaccine against pandemic influenza A (H1N1) 2009. Expert review of vaccines 10, 35–43.

[56] Miller, E., Hoschler, K., Hardelid, P., Stanford, E., Andrews, N., Zambon, M., 2010. Incidence of 2009 pandemic influenza A H1N1 infection in England: a cross-sectional serological study. The Lancet 375, 1100–1108.

[57] Miller, M.A., Viboud, C. ad Balinska, M., Simonsen, L., 2009. The signature features of influenza pandemics—implications for policy. New England Journal of Medicine 360(25), 2595–2598.

[58] Minter, A., Retkute, R., 2019. Approximate bayesian computation for infectious disease modelling. Epidemics 29, 100368.

[59] Morris, S.E., Freiesleben de Blasio, B., Viboud, C., Wesolowski, A., Bjørnstad, O.N., Grenfell, B.T., 2018. Analysis of multi-level spatial data reveals strong synchrony in seasonal influenza epidemics across Norway, Sweden, and Denmark. PloS one 13, e0197519.

[60] Mytton, O., Rutter, P., Donaldson, L., 2012. Influenza A (H1N1) pdm09 in England, 2009 to 2011: a greater burden of severe illness in the year after the pandemic than in the pandemic year. Eurosurveillance 17, 20139.

[61] NHS, 2022. Children's flu vaccine. Accessed 7/2/23.

[62] Office for National Statistics, 2019. Travelpac: travel to and from the UK, 2009-2019 edition.

[63] Prem, K., Cook, A.R., Jit, M., 2017. Projecting social contact matrices in 152 countries using contact surveys and demographic data. PLoS computational biology 13, e1005697.

[64] Rambhia, K.J., Rambhia, M.T., 2019. Early bird gets the flu: what should be done about waning intraseasonal immunity against seasonal influenza? Clinical Infectious Diseases 68, 1235–1240.

[65] Recker, M., Pybus, O.G., Nee, S., Gupta, S., 2007. The generation of influenza outbreaks by a network of host immune responses against a limited set of antigenic types. Proceedings of the National Academy of Sciences 104, 7711–7716.

[66] Rosendahl Huber, S.K., Hendriks, M., Jacobi, R.H., Van De Kassteele, J., Mandersloot-Oskam, J.C., Van Boxtel, R.A., Wensing, A.M., Rots, N.Y., Luytjes, W., Van Beek, J., 2019. Immunogenicity of influenza vaccines: evidence for differential effect of secondary vaccination on humoral and cellular immunity. Frontiers in immunology 9, 3103.

[67] Russell, C.A., Jones, T.C., Barr, I.G., Cox, N.J., Garten, R.J., Gregory, V., Gust, I.D., Hampson, A.W., Hay, A.J., Hurt, A.C., et al., 2008. The global circulation of seasonal influenza A (H3N2) viruses. Science 320, 340–346.

[68] Shaman, J., Kohn, M., 2009. Absolute humidity modulates influenza survival, transmission, and seasonality. Proceedings of the National Academy of Sciences 106, 3243–3248.

[69] Skowronski, D.M., Woolcott, J.C., Tweed, S.A., Brunham, R.C., Marra, F., 2006. Potential cost-effectiveness of annual influenza immunization for infants and toddlers: experience from Canada. Vaccine 24, 4222–4232.

[70] Sparrow, E., Wood, J.G., Chadwick, C., Newall, A.T., Torvaldsen, S., Moen, A., Torelli, G., 2021. Global production capacity of seasonal and pandemic influenza vaccines in 2019. Vaccine 39, 512–520.

[71] Ssentongo, P., Ssentongo, A.E., Voleti, N., Groff, D., Sun, A., Ba, D.M., Nunez, J., Parent, L.J., Chinchilli, V.M., Paules, C.I., 2022. Sars-cov-2 vaccine effectiveness against infection, symptomatic and severe covid-19: a systematic review and meta-analysis. BMC infectious diseases 22, 1–12.

[72] Steel, J., Palese, P., Lowen, A.C., 2011. Transmission of a 2009 pandemic influenza virus shows a sensitivity to temperature and humidity similar to that of an H3N2 seasonal strain. Journal of virology 85, 1400.

[73] Suptawiwat, O., Kongchanagul, A., Boonarkart, C., Auewarakul, P., 2018. H1N1 seasonal influenza virus evolutionary rate changed over time. Virus research 250, 43–50.

[74] Tamerius, J.D., Shaman, J., Alonso, W.J., Bloom-Feshbach, K., Uejio, C.K., Comrie, A., Viboud, C., 2013. Environmental predictors of seasonal influenza epidemics across temperate and tropical climates. PLoS Pathog 9, e1003194.

[75] Towers, S., Geisse, K.V., Tsai, C.C., Han, Q., Feng, Z., 2012. The impact of school closures on pandemic influenza: Assessing potential repercussions using a seasonal SIR model. Mathematical Biosciences & Engineering 9, 413.

[76] Tregoning, J.S., Russell, R.F., Kinnear, E., 2018. Adjuvanted influenza vaccines. Human vaccines & immunotherapeutics 14, 550–564.

[77] Truscott, J., Fraser, C., Cauchemez, S., Meeyai, A., Hinsley, W., Donnelly, C.A., Ghani, A., Ferguson, N., 2012. Essential epidemiological mechanisms underpinning the transmission dynamics of seasonal influenza. Journal of The Royal Society Interface 9, 304–312.

[78] Truscott, J., Fraser, C., Hinsley, W., Cauchemez, S., Donnelly, C., Ghani, A., Ferguson, N., Meeyai, A., 2009. Quantifying the transmissibility of human influenza and its seasonal variation in temperate regions. PLoS currents 1.

[79] UK Office for National Statistics, 2009. United Kingdom population mid-year estimate.

[80] UKHSA, 2023. Investigation into the risk to human health of avian influenza (influenza A H5N1) in England: technical briefing 2. Accessed 27/2/23.

[81] Valkenburg, S.A., Leung, N.H., Bull, M.B., Yan, L.m., Li, A.P., Poon, L.L., Cowling, B.J., 2018. The hurdles from bench to bedside in the realization and implementation of a universal influenza vaccine. Frontiers in Immunology 9, 1479.

[82] Van Kerkhove, M.D., Mounts, A.W., 2011. 2009 versus 2010 comparison of influenza activity in southern hemisphere temperate countries. Influenza and other respiratory viruses 5, 375.

[83] Viboud, C., Grais, R.F., Lafont, B.A., Miller, M.A., Simonsen, L., 2005. Multinational impact of the 1968 Hong Kong influenza pandemic: evidence for a smoldering pandemic. The Journal of infectious diseases 192, 233–248.

[84] Wang, M., Yuan, J., Li, T., Liu, Y., Wu, J., Di, B., Chen, X., Xu, X., Lu, E., Li, K., et al., 2011. Antibody dynamics of 2009 influenza A (H1N1) virus in infected patients and vaccinated people in China. PloS one 6, e16809.

[85] de Whalley, P.C., Pollard, A.J., 2013. Pandemic influenza A (H1N1) 2009 vaccination in children: A UK perspective. Journal of paediatrics and child health 49, E183–E188.

[86] World Health Organisation, 2014. Flunet.

[87] World Health Organization and others, 2014. Recommended composition of influenza virus vaccines for use in the 2014-2015 northern hemisphere influenza season. Weekly Epidemiological Record= Relevé épidémiologique hebdomadaire 89, 93–104.

[88] Zhang, Z., Mateus, J., Coelho, C.H., Dan, J.M., Moderbacher, C.R., Gálvez, R.I., Cortes, F.H., Grifoni, A., Tarke, A., Chang, J., et al., 2022. Humoral and cellular immune memory to four covid-19 vaccines. Cell 185, 2434–2451.

[89] Zhu, F.C., Wang, H., Fang, H.H., Yang, J.G., Lin, X.J., Liang, X.F., Zhang, X.F., Pan, H.X., Meng, F.Y., Hu, Y.M., et al., 2009. A novel influenza A (H1N1) vaccine in various age groups. New England Journal of Medicine 361, 2414–2423.